Available online at www.sciencedirect.com
ScienceDirect
Optical Materials 29 (2007) 532–538
OPTICAL Materials
www.elsevier.com/locate/optmat

# Hydrothermal synthesis and photoluminescent properties of ZnO sub-micrometer and micrometer rods

Libo Fan, Hongwei Song *, Lixin Yu, Zhongxin Liu, Linmei Yang, Guohui Pan, Xue Bai, Yanqiang Lei, Tie Wang, Zhuhong Zheng, Xianggui Kong

*Key Laboratory of Excited State Physics, Changchun Institute of Optics, Fine Mechanics and Physics, Chinese Academy of Sciences, 16 Eastern South-Lake Road, Changchun 130033, PR China*

Received 2 March 2005; accepted 6 August 2005
Available online 18 January 2006

**Abstract**

ZnO sub-micrometer and micrometer rods with hexagonal structure were synthesized by the hydrothermal method and characterized by X-ray diffraction (XRD) patterns, scanning electron microscopy (SEM) images and Raman spectra. Their luminescent properties including room-temperature emission spectra, fluorescent dynamics and temperature dependence of luminescence were studied. The results indicated that, as $Zn(NO_3)_2 \cdot 6H_2O$ and NaOH satisfied the stoichiometric ratio (1:2) in precursor solution, the ZnO rods were with an average diameter of 100 nm and length of 1 μm. As NaOH was insufficient or excessive, both diameter and length of the rods increased significantly. And more, a large number of defect states were involved, which greatly affected the photoluminescent properties of ZnO rods. The ultraviolet (UV) emission of excitons (3.2 eV) and visible emission (2.0 eV) from deep levels (DLs) of defects were observed. As NaOH was insufficient or excessive, the relative intensity of the defect emission increased, while that of the exciton emission decreased. The lifetimes of the excitons decreased with the increase of DLs. Two decay components were observed for the fluorescent dynamics of DLs. According to temperature-dependent luminescence, some important parameters were obtained and compared, such as the Einstein temperature for the excitons, the thermal activation energy of excitons or DLs etc.


*PACS:* 78.55.Et; 61.46.+w; 33.50.Dq

## 1. Introduction

As a wide direct band gap (~3.3 eV) semiconductor, ZnO has been attracting much attention due to its potential applications in short-wavelength UV laser and blue–green optoelectronic devices [1–7]. The large exciton binding energy (~60 meV) permits exiton recombination well above room temperature [8–10]. Laser under optical excitation has been experimentally demonstrated at room temperature [3–7]. Recently, one-dimensional (1-D) structures, such as nanowires, nanorods and nanotubes have aroused remarkable attention due to a great deal of potential applications in data storage, advanced catalyst, photoelectronic devices etc. [11,12]. Moreover, in comparison with zero-dimensional (0-D) structures, the space anisotropy of 1-D structures provides a better model system to study the dependence of electronic transport, optical and mechanical properties on size confinement and dimensionality [6,13]. As an important photoelectronic material, 1-D ZnO nanomaterials also attracted extensive interests in the past decade. Especially, UV-nanowire laser under optical excitation in ZnO was realized at room temperature by Yang et al. in 2001 [6].

Up to now, different techniques have been used to prepare 1-D nanocrystalline ZnO, such as electrodeposition method, vapor transport method, vapor deposition method, vapor–liquid–solid process, wet chemical method and so on [14–20]. It is conceived that preparation of 1-D ZnO nanostructures via wet chemical routes without

* Corresponding author. Tel./fax: +86 431 6176320.
*E-mail address:* songhongwei2000@sina.com.cn (H. Song).

0925-3467/$ - see front matter © 2005 Elsevier B.V. All rights reserved.
doi:10.1016/j.optmat.2005.08.046

involving catalysts or templates provides a promising option for large-scale production of well-dispersed materials [21–24]. The photoluminescent properties of semiconductors, such as the luminescence of excitons or DLs, depend upon the preparation techniques strongly [7].

Recently, we systematically synthesized ZnO submicrometer and micrometer rods by a hydrothermal method, which was originally reported by Liu and Zeng [25]. The diameter and length of 1-D ZnO rods were modified, only by changing the concentration of NaOH solution. In this paper, we mainly reported the structural and photoluminescent properties of the ZnO rods prepared by hydrothermal method, including their Raman spectra, photoluminescence (PL), dynamics at room-temperature and temperature-dependent PL.

## 2. Experiments

### 2.1. Sample preparation

All chemicals were analytic grade reagents without further purification. In a typical synthesis, 10 mL of 1 M NaOH aqueous solution was added into 10 mL of 1 M $Zn(NO_3)_2 \cdot 6H_2O$ aqueous solution at room temperature under magnetic stir. When white suspension formed, 60 mL of ethanol was introduced under stir for 10 min. The resultant suspension was transferred into five 25 mL Teflon-lined stainless steel autoclaves averagely, and maintained at 180 °C for 20 h. After the reaction, the Teflon-lined autoclaves were cooled naturally to room temperature. Then the white precipitate was collected and washed with deionized water and ethanol for several times to remove the ions possibly remaining in the final products. Finally, the white product (ZnO rods, **a**) was obtained by centrifugation and dried at 80–90 °C for 12 h in a vacuum condition. As comparison, three other similar experiments have also been performed, only by changing the concentration of NaOH solution. The concentration of 10 mL NaOH aqueous solution was changed from 1 M for **a** to 2 M, 8 M, 10 M for **b**, **c**, **d**, and 1 M $Zn(NO_3)_2 \cdot 6H_2O$ aqueous solution was 10 mL for all samples. Therefore, the concentration ratios of $Zn(NO_3)_2 \cdot 6H_2O$ to NaOH for **a, b**, **c**, **d** were 1:1, 1:2, 1:8, 1:10, respectively.

### 2.2. Measurements

All samples were characterized by XRD using a rotating anode X-ray diffractometer with CuKα radiation ($\lambda = 1.5405$ Å). Raman spectra were measured by a LabRam Raman Spectrometer (Jobin–Yvon Company, France). A 488-nm continuous argon ion laser was used as scattering light source. Photoluminescent spectra were measured by the same LabRam Raman Spectrometer under the excitation of a 325-nm He–Cd laser source. In the measurements of the temperature dependence of PL, the samples were put into a cryogenic unit cooled by liquid nitrogen, in which the temperature varied from 78 K to room temperature. Fluorescent dynamics were measured on an FL920-Fluorescence Lifetime Spectrometer (Edinburgh Instruments) with MCP-PMT. The excitation source was an optical parametric amplifier (OPA) pumped by a Ti/sapphire regeneration amplifier (Spectra Physics Co. Ltd.), which provided a 130 fs full width at half maximum (FWHW) pulse (wavelength of 345 nm, repetition rate of 1 kHz).

## 3. Results and discussion

### 3.1. Sample characterization

The XRD patterns of different ZnO samples were shown in Fig. 1. As seen, all the samples were well crystallized. All diffraction peaks in the XRD patterns of all ZnO samples can be indexed as the pure hexagonal structure, which are consistent with the results in the standard card (JCPDS 05-0664). Apparently, the diffraction peaks in the range of 30–40° (2$\theta$, the 100, 002 and 101 facets) had a little variation in different samples. The lattice constants ***a*** and ***c*** in all samples were calculated according to the diffraction locations of 100 and 102 facets, respectively, which were listed in Table 1. In the standard bulk ZnO powders, lattice constants ***a*** and ***c*** are 3.249 Å and 5.205 Å, respectively. The values of lattice constants ***a*** and ***c*** in these hydrothermal synthesized ZnO powders decreased at different extent in comparison to the bulk powders.

Fig. 2 shows the SEM images of all samples. It can be seen that rod-like ZnO powders formed in all the samples. The diameter and length of the rods varied with different preparation conditions. As $Zn(NO_3)_2 \cdot 6H_2O$ and NaOH satisfied the stoichiometric ratio (1:2), the average diameter of the rods was 100 nm and length was 0.8 μm. As NaOH was insufficient or excessive, the aspect ratio varied little but the diameter and length both increased. The average diameter and length of the ZnO rods in different samples were also listed in Table 1.

Fig. 3 shows the Raman spectra for different ZnO samples. In the figure, the vibrational peaks at 332, 383, 438, 583, 987, 1101 and 1154 $cm^{-1}$ appeared. All these peaks

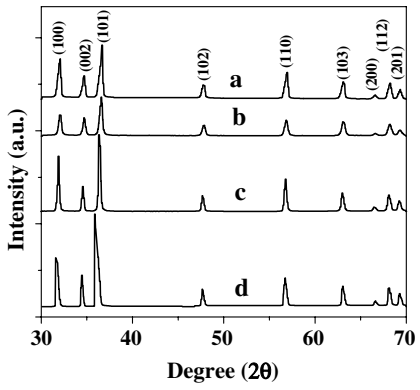


Fig. 1. XRD patterns of different ZnO rods.

Table 1
Lattice constants, sizes and decay time constants for different samples

| Sample | Lattice constant | | Morphology: nanorods | | Lifetime | | | |
|---|---|---|---|---|---|---|---|---|
| | *a* (Å) | *c* (Å) | Size | | Exciton emission | Deep-level emission | | |
| | | | Diameter (nm) | Length (μm) | $\tau$ (ps) | $\tau_1$ (ns) | $\tau_2$ (ns) | $R_2$ (%) |
| **a** | 3.248 | 5.193 | ~300 | ~1.2 | 101 | 0.35 | 7.4 | 8 |
| **b** | 3.244 | 5.194 | ~100 | ~0.8 | 144 | 0.28 | 4.7 | 6 |
| **c** | 3.245 | 5.198 | ~300 | ~3.0 | 30 | 0.20 | 15.3 | 15 |
| **d** | 3.239 | 5.196 | ~1000 | ~10.0 | 40 | 1.3 | 20.6 | 33 |

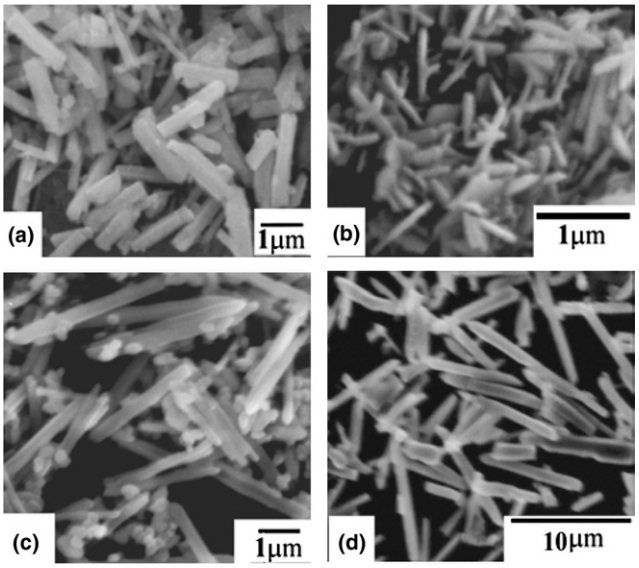


Fig. 2. SEM images of different ZnO rods.

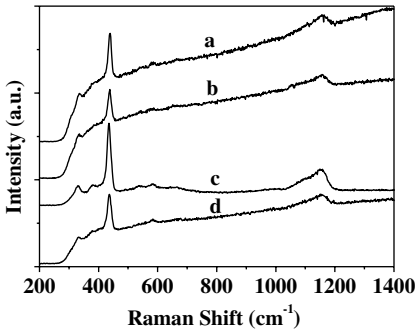


Fig. 3. Raman spectra of different ZnO rods excited by a 488-nm laser.

were assigned on the basis of group theoretical analysis. The results as well as a comparison with previous works were listed in Table 2, from which a good agreement was evident [26–28].

### 3.2. Photoluminescent spectra and dynamics at room temperature

Fig. 4 shows the photoluminescent spectra for different ZnO powders at room temperature under a 325-nm excitation. It can be seen that all samples have two emission peaks, a narrow peak at ~3.2 eV and a broad peak at ~2.0 eV. The near-UV peak at 3.2 eV (~380 nm) originates from the recombination of excitons [29], while the peak at 2.0 eV (~600 nm) from the recombination emission between the conduction band or shallow donors and interstitial oxygen ($O_i$), which acts as deep-level (DL) $O_i$ center [30,31]. For **a** and **b**, the UV-exciton emissions were stronger than the visible emissions originated from the recombination of oxygen defects. For **c** and **d**, the exciton emissions became much weaker than the visible emissions. In the other words, the more the oxygen defects are, the less the excitons are. This suggests that, when they are excited, excitons could be captured by the DL defects, which leads to the quenching of the exciton emission and the enhancement of the emission originated from the recombination of the oxygen defects [7]. This conclusion was also proved further by the following dynamics of fluorescence. It should be mentioned here that the main near-UV peak for **d**, in comparison to other samples, shifted to the lower energy side and a shoulder appeared at the higher energy side of the main peak. Therefore, the global FWHW become broad. This can be attributed to the existence of more types of excitons in the sample **d**.

Fig. 5(a) and (b) shows the fluorescent dynamics of the exciton and the defect emission, respectively. The fluorescent lifetimes for excitons and DLs were obtained by fitting and listed in Table 1. It can be seen from Fig. 5(a) that the exciton-emission decays deviated from exponential rule. The exciton lifetimes in different ZnO rods varied from 30 ps to 144 ps (see Table 1), which agreed with the reported results (50–300 ps) of bound-exiton lifetime in bulk ZnO [32]. Decays of the exciton emissions in **a** and **b** were slow, while in **c** and **d** were fast. The fluorescence decay is dominated by radiative decay of the excitons and various nonradiative processes such as captured by DL traps, low-lying surface states, and multiphonon scattering [33]. According to the emission spectra in Fig. 4, more defect states were involved in **c** and **d** in comparison to **a** and **b**. This will lead the nonradiative relaxation to increase. As a consequence, the exciton decay becomes fast. In Fig. 5(b), there existed two decay components for the defects emission, a fast one and a slow one. The relative proportions of the slow process ($R_2$) in **a** and **b** were very small and nearly the same, but increased greatly in **c** and **d** (see Table 1). The existence of two decay components suggests that two kinds of defect states were involved.

Table 2
Wavenumber (in $cm^{-1}$) and symmetries of the modes found in Raman spectra and their assignments

| Wave number | Symmetry | Process | Ref. [26] | Ref. [27] | Ref. [28] | My result |
|---|---|---|---|---|---|---|
| 331 | $A_1$ | Acoust. overtone | 331 | | | 332 |
| 383 | $A_1$ (TO) | First progress | 383 | 381 | 397 | 383 |
| 410 | $E_1$ (TO) | First progress | | 407 | 426 | |
| 438 | $E_2$ | First progress | 438 | 441 | 449 | 438 |
| 540 | $A_1$ (LO) | First progress | 549 | | 559 | |
| 584 | $E_1$ (LO) | First progress | 584 | 583 | 577 | 583 |
| 660 | $A_1$ | Acoust. overtone | 660 | | | |
| 776 | $A_1$, $E_2$ | Acoust. opt. comp. | | | | |
| 987 | $A_1$, $E_2$ | Opt. comp. | | | | 987 |
| 1101 | $A_1$, $E_2$ | Acoust. comp. | | | | 1101 |
| 1154 | $A_1$ | Opt. overtone | | | | 1154 |

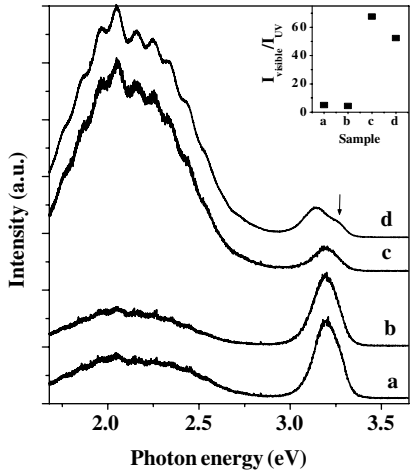


Fig. 4. Photoluminescent spectra of different ZnO rods excited by a 325-nm laser at room temperature. Insert: the ratios of integral intensity of the visible to the UV emission for **a**, **b**, **c**, **d**.

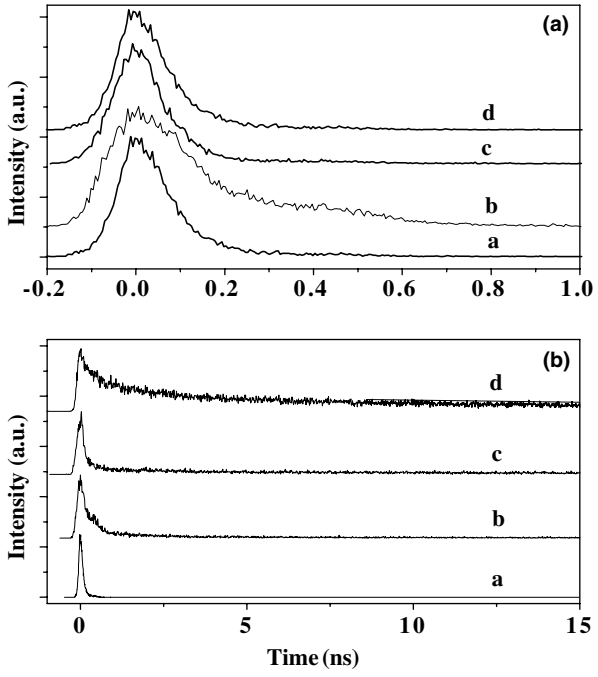


Fig. 5. Fluorescent decay curves of (a) exciton emission at 392 nm and (b) defect emission at 600 nm.

The long-lived defect states in **c** and **d** increased more greatly than those in **a** and **b**.

### 3.3. Temperature dependence of photoluminescent spectra

As shown in Fig. 6(a) and (b), the temperature dependence of PL for **b** and **c,** as the examples of the ZnO rods containing less and more defect states, were studied respectively. It can be seen that, with increasing temperature, the main exciton-emission location red shifted, while the intensity decreased and the FWHM became broad for the both samples. For **b**, a low shoulder (3.22 eV) appeared at low energy side of the main exciton peak (3.28 eV) at low temperature and decreased gradually with increasing temperature. It disappeared completely around 200 K. The shoulder may come from the emission of some bound excitons. For **c**, the shoulder did not appear. This was attributed to the strong energy transfer from the excitons at 3.22 eV to the defect states.

The energies of the exciton emissions for **b** and **c** were plotted as a function of temperature, as shown in Fig. 7.

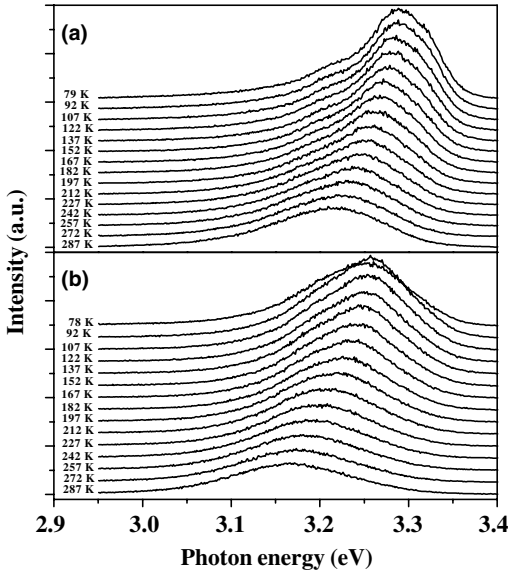


Fig. 6. Temperature dependence of photoluminescent spectra for (a) sample **b** and (b) sample **c,** excited by a 325-nm laser.

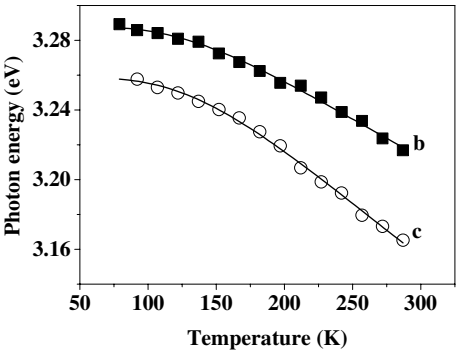


Fig. 7. Peak energy of the exciton emission as a function of temperature. The scattered dots are the experimental data and solid lines are fitting functions.

It can be seen that for the both samples, the transition energies decreased with increasing temperature and changed more rapidly for **c**. Considering the exciton–phonon interaction, the exciton energy as a function of temperature obeys the Bose–Einstein relation [34],

$$E(T) = E_0 - A/[\exp(\Theta_E/T) - 1], \quad (1)$$

where $E_0$ is the transition energy of excitons at 0 K, $A$ is the proportional coefficient, $\Theta_E$ is the Einstein characteristic temperature and $T$ is the absolute temperature. By fitting, $E_0$ was determined to be 3.289 eV for **b** and 3.260 eV for **c**, $A$ to be 0.24 for **b** and 0.36 for **c**, $\Theta_E$ to be 427 K (44.6 meV) for **b** and 443 K (45.8 meV) for **c**. The values of $E_0$ are smaller than that assigned to the free excitons reported in bulk or thin-film ZnO (~3.37 eV) [35–37]. Presently, the lattice constants for the ZnO rods are close to the standard ZnO powders, and the size confinement effect should not work at all. Thus the band gap or free-exciton energy in ZnO rods should be close to that in the bulk one, i.e. 3.37 eV [35]. Although the fitting was taken in a narrow temperature range (78–290 K) and the results of $E_0$ may be not so accurate, we consider that the wet chemical method may introduce various impurities unavoidably, which act as donors or acceptors in the products. The energy of free excitons which could be captured by these impurities, transformed into the luminescence of the bound excitons or defect states. Therefore we are inclined to assign the main exciton peak in ZnO rods to be the bound-exciton emission instead of the free-exciton emission and the emission originated from the free excitons was not observed. According to the fitting results, the obtained values of $\Theta_E$ for **b** and **c** are very close, suggesting that the modes of exciton–phonon coupling are the same. The value of $A$ for **c** is larger than that for **b**, indicating the stronger exciton–phonon interaction.

It is noted that the temperature dependence of exciton energy was also fitted by the empirical function developed by Varshni [38]. The results indicate that the Bose–Einstein fitting function is more suitable for this work. It has been shown that in polar semiconductors which have optical phonon branches energetically next to the acoustic ones. Using the empirical equation that assumes Einstein phonons to fit the variation of exciton-transition energy with temperature is better than Varshni fitting which assumes Debey phonons [34].

Fig. 8 shows the temperature dependence of the emission intensity of excitons. It can be seen that the exciton intensity decreased more rapidly for **c** than that for **b**. In the figure, the intensity as a function of temperature was fitted by the well-known thermal activation function [36],

$$I(T) = I_0/[1 + \alpha \cdot \exp(-E_A/(k_B \cdot T))], \quad (2)$$

where $I_0$ is the emission intensity at 0 K, $\alpha$ is the proportional coefficient, $E_A$ is the thermal activation energy, $k_B$ is the Boltzmann's constant and $T$ is the absolute temperature. By fitting, $I_0$ was determined to be 238 for **b** and 239 for **c**, $\alpha$ to be 2.7 for **b** and 5.9 for **c**, $E_A$ to be 32.4 meV for **b** and 41.5 meV for **c**. The values of $E_A$ obtained for the two samples are smaller than the binding energy (60 meV) of free excitons, which also suggests that the excitons do not come from the free excitons. $E_A$ for **c** is a little bit larger than that for **b**, while $\alpha$ for **c** is much lager than that for **b**.

The initial temperature (78 K) is not low enough to resolve the contributions of bound and free excitons in the near-band-edge emission in this work, however, combining the PL spectra, fitting results and the hydrothermal method and so on, we also consider that the main exciton

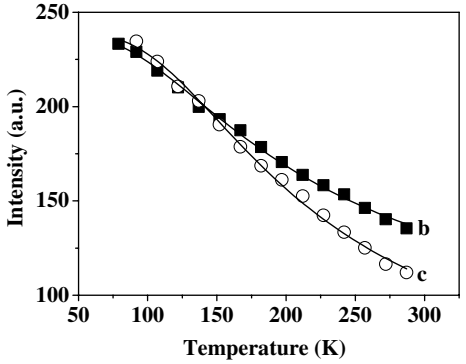


Fig. 8. The integral intensity of the exciton peak as a function of temperature. The scattered dots are the experimental data and solid curves are the fitting functions.

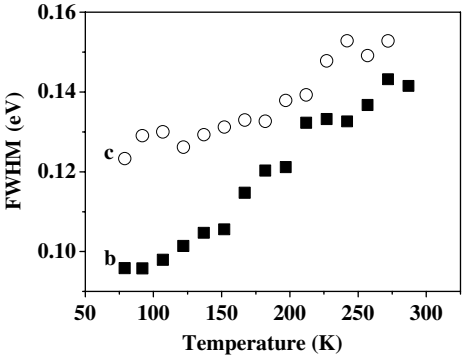


Fig. 9. FWHM of the exciton emission as a function of temperature.

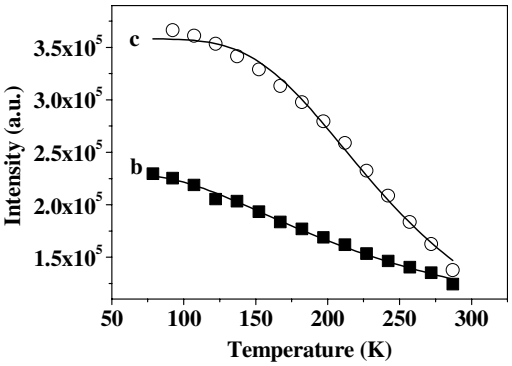


Fig. 10. The integral intensity of the deep-level peak as a function of temperature. The scattered dots are the experimental data and solid curves are the fitting functions.

peaks in ZnO rods should be assigned to the bound-exciton emission instead of the free-exciton emission.

Fig. 9 shows the dependence of FWHM of the exciton emission on temperature. It can be seen that for the both samples, the FWHM increased with the elevating temperature. The FWHM for **c** is broader than that for **b** at any temperature, suggesting that there existed more types of structure or point defects in **c** than that in **b**. This was consistent with the dynamics results that the exciton-emission lifetime for **c** decreased more quickly than that for **b**.

Fig. 10 shows the dependence of the emission intensity of the DL peaks as a function of temperature. It can be seen that the emission intensity of the DL peaks decreased with elevating temperature for both the samples, which was just like the situation in the bulk ZnO reported previously [39]. For **c**, the intensity changed more rapidly. The intensity as a function of temperature was also well fitted by Eq. (2). By fitting, $I_0$ was determined to be $2.3 \times 10^5$ for **b** and $3.6 \times 10^5$ for **c**, $\alpha$ to be 3.9 for **b** and 47.2 for **c**, $E_A$ to be 39.7 meV for **b** and 86.4 meV for **c**. The thermal activation energy for **c** is much larger than that for **b.** This is due to a large number of long-lived defect states involved in **c,** as discussed by fluorescent dynamics. The long-lived defect states should have smaller nonradiative relaxation rate and larger thermal activation rate than that of the short-lived defect states.

## 4. Conclusions

In summary, ZnO sub-micrometer and micrometer rods with hexagonal structure were synthesized by the hydrothermal method. As $Zn(NO_3)_2 \cdot 6H_2O$ and NaOH satisfied the stoichiometric ratio (1:2), the ZnO rods were with an average diameter of 100 nm and length of 0.8 μm. As NaOH was insufficient or excessive, both diameter and length of the rods increased significantly. And more, a large number of defect states were involved, which influenced the photoluminescent properties of ZnO rods significantly. The UV emission coming from the bound excitons (3.2 eV) and visible emission (2.0 eV) coming from the DLs were observed in all the samples. As NaOH was excessive (**c** and **d**), the intensity of the defect emission increased largely, while those of the exciton emission decreased at room temperature. The lifetimes of the excitons varied from 30 ps to 144 ps at room temperature. The stronger the emission of the DLs was, the shorter the exciton lifetime was, indicating the nonradiative relaxation of the excitons to the DLs. Two decay components were observed for the fluorescent dynamics of DLs. One lifetime varied from one hundred to several hundreds ps and another one varied from several to 20 ns. The stronger the emission of DLs was, the larger the component with long lifetime was, suggesting long-lived DLs were involved largely in the NaOH-excessive samples. As a function of temperature the exciton energy was fitted by Bose–Einstein relation, while the intensity was fitted by the thermal activation relationship, for the both samples containing less and excessive DLs. These results indicated that the exciton–phonon interaction and the thermal quenching became stronger for the DLs-excessive samples. The thermal activation energies of the excitons for **b** (less defects) and **c** (more defects) were 32.4 and 41.5 meV, respectively. The intensity variation of the DL emissions also obeyed the thermal activation relationship, with thermal activation energies of 39.7 and 86.4 meV for **b** and **c** respectively.

## Acknowledgments

The authors gratefully thank the financial supports of Nation Natural Science Foundation of China (Grant No. 10374086) and Talent Youth Foundation of Jilin Province (Grant No. 20040105). We also thank Ligong Zhang and Zhiyan Xiao for their helpful discussion.

## References

[1] R.F. Service, Science 276 (1997) 895.
[2] C.M. Lieber, Solid State Commun. 107 (1998) 607.
[3] Z.K. Tang, G.K.L. Wang, P. Yu, M. Kawasaki, A. Ohtomo, H. Koinuma, Y. Segawa, Appl. Phys. Lett. 72 (1998) 3270.
[4] H. Cao, Y.G. Zhao, S.T. Ho, E.W. Seelig, Q.H. Wang, R.P.H. Chang, Phys. Rev. Lett. 82 (1999) 2278.
[5] S.F. Yu, C. Yuen, S.P. Lau, W.I. Park, G.C. Yi, Appl. Phys. Lett. 84 (2004) 3241.
[6] M. Huang, S. Mao, H. Feick, H. Yan, Y. Wu, H. Kind, E. Weber, R. Russo, P. Yang, Science 292 (2001) 1897.
[7] Z. Qiu, K.S. Wong, Appl. Phys. Lett. 84 (2004) 2739.
[8] M. Zamfirescu, A. Kavokin, B. Gil, G. Malpuech, M. Kaliteevzki, Phys. Rev. B 65 (2002) 161205-1.
[9] J.-J. Wu, S.-C. Liu, Adv. Mater. 14 (2002) 215.
[10] W. Park II, G.-C. Yi, M. Kim, S.J. Pennycook, Adv. Mater. 14 (2002) 1841.
[11] S. Lijima, Nature (London) 354 (1991) 56.
[12] X.F. Daun, Y. Huang, Y. Cui, J.F. Wang, C.M. Lieber, Nature (London) 409 (2001) 66.
[13] Y. Xia, P. Yang, Adv. Mater. 15 (2003) 351.
[14] R. Konenkamp, K. Boedecher, M.C. Lux-Steiner, M. Poschenrieder, F. Zenia, C.L. Clement, S. Wagner, Appl. Phys. Lett. 77 (2000) 2575.
[15] M.H. Huang, Y.Y. Wu, H. Feick, N. Tran, E. Weber, P.D. Yang, Adv. Mater. 13 (2001) 113.
[16] Y.C. Kong, D.P. Yu, B. Zhang, W. Fang, S.Q. Feng, Appl. Phys. Lett. 78 (2001) 407.

[17] S.C. Lyu, Y. Zhang, H. Ruh, H.-J. Lee, H.-W. Shim, E.-K. Suh, C.J. Lee, Chem. Phys. Lett. 363 (2002) 134.
[18] Y. Li, P. Lin, C.Y. Lee, T.Y. Tseng, C.J. Huang, J. Phys. D: Appl. Phys. 37 (2004) 2274.
[19] Y. Li, G.W. Meng, L.D. Zhang, F. Phillipp, Appl. Phys. Lett. 76 (2000) 2011.
[20] B. Liu, H.C. Zeng, Langmuir 20 (2004) 4196.
[21] X.Y. Zhang, J.Y. Dai, H.C. Ong, N. Wang, H.L.W. Chan, C.L. Choy, Chem. Phys. Lett. 393 (2004) 17.
[22] J. Wang, L. Gao, J. Mater. Chem. 13 (2003) 2551.
[23] X. Wang, Y.D. Li, J. Am. Chem. Soc. 41 (2002) 2446.
[24] T. Kasuga, M. Hiramatsu, A. Hoson, T. Sekino, K. Nihara, Adv. Mater. 11 (1999) 1307.
[25] B. Liu, H.C. Zeng, J. Am. Chem. Soc. 125 (2003) 4430.
[26] G. Xu, P. Jin, Phys. Rev. B 69 (2004) 113303.
[27] R.H. Callender, S.S. Sussman, M. Selders, R.K. Chang, Phys. Rev. B 7 (1973) 3788.
[28] F. Decremps, J.P. Porres, A.M. Saitta, J.C. Chervin, A. Polian, Phys. Rev. B 65 (2002) 092101.
[29] T.W. Kim, T. Kawazoe, S. Yamazaki, M. Ohtsu, T. Sekiguchi, Appl. Phys. Lett. 84 (2004) 3358.
[30] A.B. Djurisic, Y.H. Leung, W.C.H. Choy, K.W. Cheah, W.K. Chah, Appl. Phys. Lett. 84 (2004) 2635.
[31] X.L. Wu, G.G. Siu, C.L. Fu, H.C. Ong, Appl. Phys. Lett. 78 (2001) 2285.
[32] J. Wilkinson, K.B. Ucer, R.T. Williams, Radiat. Meas. 38 (2004) 501.
[33] S. Hong, T. Joo, W. Park II, Y.H. Jun, G.C. Yi, Appl. Phys. Lett. 83 (2003) 4157.
[34] A. Setoguchi, H. Nakanishi, Appl. Phys. Lett. 76 (2000) 1576.
[35] H. Alves, D. Pfisterer, A. Zeuner, T. Riemann, J. Christen, D.M. Hofmann, B.K. Meyer, Opt. Mater. 23 (2003) 33.
[36] B.S. Li, Y.C. Liu, Z.Z. Zhi, D.Z. Shen, Y.M. Lu, J.Y. Zhang, X.W. Fan, J. Cryst. Growth 240 (2002) 479.
[37] S.F. Chichibu, T. Sota, P. Fons, K. Iwata, A. Yamada, K. Matsubara, S. Niki, Jpn. J. Appl. Phys. 41 (2002) L935.
[38] Y.P. Varshni, Physica (Amsterdam) 34 (1967) 149.
[39] S.S. Chang, G.J. Choi, H.J. Park, M.E. Stora, R.E. Hummel, Mater. Sci. Engrg. B 83 (2001) 29.